Journal of Scientific & Industrial Research
Vol. 67, June 2008, pp. 421-427

Cutting force prediction model by FEA and RSM when machining Hastelloy C-22HS with 90° holder

K Kadirgama[1], K A Abou-El-Hossein[2], B Mohammad[3], Habeeb AL-Ani[3] and M M Noor[1]

[1]Department of Mechanical Engineering, University Malaysia Pahang, 25000, Kuantan Pahang, Malaysia

[2]Mechanical Engineering Department, Stellenbosch University, South Africa

[3]Department of Mechanical Engineering, University Tenaga Nasional

Received 20 June 2007; revised 03 April 2008; accepted 04 April 2008

Finite element (FEA) method and response surface method (RSM) are used to find the effect of milling parameters (cutting speed, feed rate and axial depth) on cutting force when milling Hastelloy C-22HS. Based on variance analyses of First- and Second-Order RSM models, most influential design variable is feed rate. Optimized cutting force values are subsequently obtained from model equations. FEA model shows distribution of cutting force.

Keywords: Cutting force, Finite element analysis Milling, Response surface method

Introduction

Corrosion-resistant high alloy castings are often the subject of major concern because failures of cast components have led to significant downtime costs and operating problems[1]. With its considerable industrial benefit as an effluent coolant, seawater remains a corrosive environment to many structural materials such as in marine and power generation sector. Hastelloy C-22HS is one of the best alloys for seawater resistance.

Allauddin *et al*[2] investigated the effect of cutting speed, feed rate and axial depth on cutting force. Trent[3] reported that decrease in cutting force due to increase in cutting speed was in-part due to softening of work piece under high-temperature generated during cutting. According to Chen[4], during finishing operation of hardened steel, radial thrust force (F_y) became largest among three cutting force components and was most sensitive to changes of cutting edge chamfer, tool nose radius and flank wear. Koenigsberger & Sabberwal[5] developed equations for milling forces using mechanistic modeling[6-10]. Another alternative is to use mechanics of cutting approach in determining milling force coefficients[11]. Cutting forces[12] are mainly affected by cutting speed, feed rate, undeformed chip thickness, cutting tool material, tool geometry (approaching angle, rake angle, etc.), depth of cut and tool wear. Taylor[13] determined values of cutting force components and Victor[14,15] and Kienzle[16] reported specific cutting coefficient tables by using different rake angles, feed and speeds and offered applicable practical equations.

*Author for correspondence
E-mail: kumaran@ump.edu.my

Box – Behnken Design and Finite Element Analysis (FEA)

Box-Behnken Design do not have axial points, thus all design points fall within the safe operation. It also ensures that all factors are never set at their high levels simultaneously[17-19]. To simulate complex procedure of metal cutting with Finite Element Model (FEM), following assumptions are used to define the problem to be solved as well as to apply boundary and loading conditions[20]: i) Cutting speed is constant; ii) Width of cut is larger than feed (plane strain condition), and both are constant; iii) Cutting velocity vector is normal to cutting edge; iv) Work piece material is a homogeneous polycrystalline, isotropic, and incompressible solid; v) Work piece is at a reference temperature (20°C) at the beginning of simulation; vi) Machine tool is perfectly rigid and no influence of machine tool dynamics on machining is considered; and vii) Constant friction at tool-chip interaction and tool-work piece interaction.

This study, using FEM and Response Surface Method (RSM), presents effect of three milling parameters (cutting speed, feed rate and axial depth) on cutting force.

Experimental Setup

Experiments (15) were carried out on Okuma CNC machining centre MX-45 VA with 90° holders and using a water-soluble coolant. Each experiment was stopped after 90 mm cutting length. To measure cutting force, 3-axis dynamometer was used. Each experiment was repeated thrice using a new cutting edge every time for accurate readings of cutting force. A cutting pass was conducted in such a way that a shoulder (depth 1-2 mm, width 3.5 mm) was produced.

Workpiece material (Hastelloy C-22HS) represents major group of workpiece materials used in industry. At room temperature, physical properties of workpiece material were as follows: density, 0.6 g/m^3; thermal conductivity, 11.8 W/m °C; mean coefficient of thermal expansion, 11.6 μm/m °C; thermal diffusivity, 0.0334 cm^2/s; specific heat, 412 J/kg °C; and Young Modulus, 223 GPa. Chemical components of Hastelloy C-22HS were: Ni, 56.60; Cr; 21.00; Mo; 17.00; Fe, 2.00; Co, 1.00; W, 1.00; Mn, 0.80; Al, 0.50; Si, 0.08; C, 0.01; & B, 0.01 %.

Cutting tools were a 12° rake positive end milling cutter (diam 50 mm). End mill can be equipped with four inserts whose only one edge can be used for cutting. Tool inserts were made by Kennametal [ISO: SPHX1205ZCFRGN1W (KC520M)]. One insert per one experiment was mounted on cutter. Cutting tool has: code name, KC520M; substrate composition, (Co, 6; Cr3C2, 0.5; WC, 93.5%); hardness (HRA), 92; coating, PVD TiALN; and thickness, 3.5 μm.

Results and Discussion

Development of First Order Cutting Force Model using RSM

After conducting first passes (one pass, 90 mm long) of 15 experiments, cutting force readings were used (method of least squares using Minitab was used for calculations) to find parameters appearing in postulated First Order Model (FOM) as

$$y' = -785.89 - 1.88x_1 + 5706.03x_2 + 578.33x_3 \quad \ldots(1)$$

From Eq. (1) response y' (cutting force) is affected significantly by feed rate followed by axial depth and cutting speed for all the models. Increase in feed rate, axial depths will cause cutting force to become larger[21]. On the other hand, decrease in cutting speed will slightly cause a reduction in cutting force[22]. Cutting tool at high cutting force is severely damaged if compared with cutting tool at low cutting force (Figs 1 and 2). Cutting tool at low cutting force can continue more than one pass while cutting tool at high force cannot continue, since it get damaged at first pass. Since nickel alloys work harden rapidly, once milling cutter starts cutting, it will become more and more difficult for further machining due to hardening effect. When cutting edge is not sharp enough, metal is pushed instead of cut, resulting in higher cutting force and higher temperature[23]. At relatively high cutting speeds (150 m/min), energy input to the system and stresses are correspondingly higher and lead to increased heat generation. The generated heat in shear zone helps to plasticize (soften) workpiece material, reducing forces required to cut material. At lower cutting speeds (100 and 125 m/min), less heat is generated and temperature-induced softening of workpiece is reduced, giving rise to higher cutting forces[24].

Predicted values by FOM are found in good agreement with experimental readings (Table 1). This indicates that the obtained linear model is useful to predict values of cutting forces. At a level of confidence of 95%, adequacy of FOM was verified using analysis of variance (ANOVA) P value of 0.073 (> 0.05) is not found significant with the lack-of fit and F-statistic is 13.16 (Table 2). This implies that the model could fit and it is adequate[22].

The developed linear model Eq. (1) was used to plot contours of cutting force at different values of axial depth. Using cutting force contours at three different combinations of axial depths (lowest "-1", middle "0", and highest values "+1"), it is observed that reduction in cutting speed and increase in feed rate cause cutting force increase dramatically (Fig. 3). Cutting force reaches highest when all cutting conditions, except for cutting speed, are maximum (Fig. 3c)

Development of Second-Order Cutting Force Model using RSM

Second Order Model (SOM) equation was established using Box – Behnken design as

$$y'' = -1082.08 + 1.06x_1 + 6699.50x_2 + 614.75x_3 - 0.07x^2{}_1 - 2811.83x^2{}_2 + 6.99x^2{}_3 + 1.12x_1x_2 - 0.19x_1x_3 - 204.6x_2x_3 \quad \ldots(2)$$

Cutting force obtained experimentally and that predicted from Eq. (2) produce similar values (Table 1). ANOVA indicates that model is adequate as P value of lack-of-fit is not significant and F-statistic is 12.73 (Table 3). There is no interaction between variables because of P value for interaction 0.719 (>0.05).

Cutting Force prediction by Finite Element Analysis

Experimental results (Fig. 4) are found not as closer as RSM 2nd model due to inadequate friction modeling

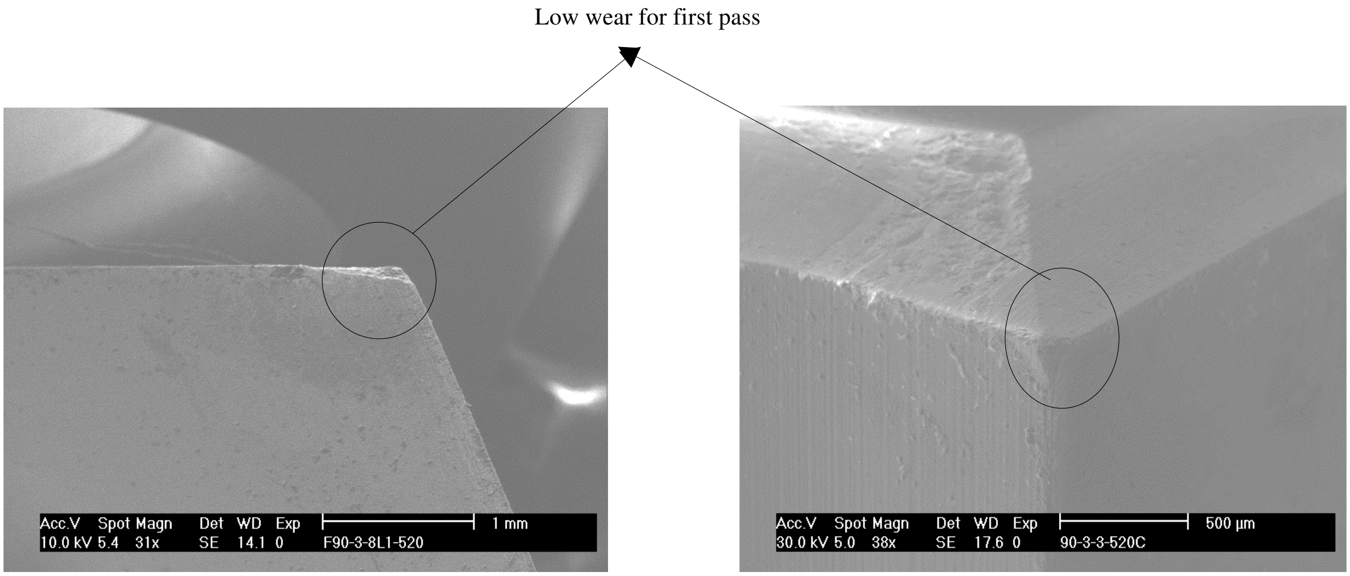

Fig. 1—SEM picture for different cutting speed (Feed rate 0.15 mm/rev, axial depth 1 mm): Cutting speed 180 m/min

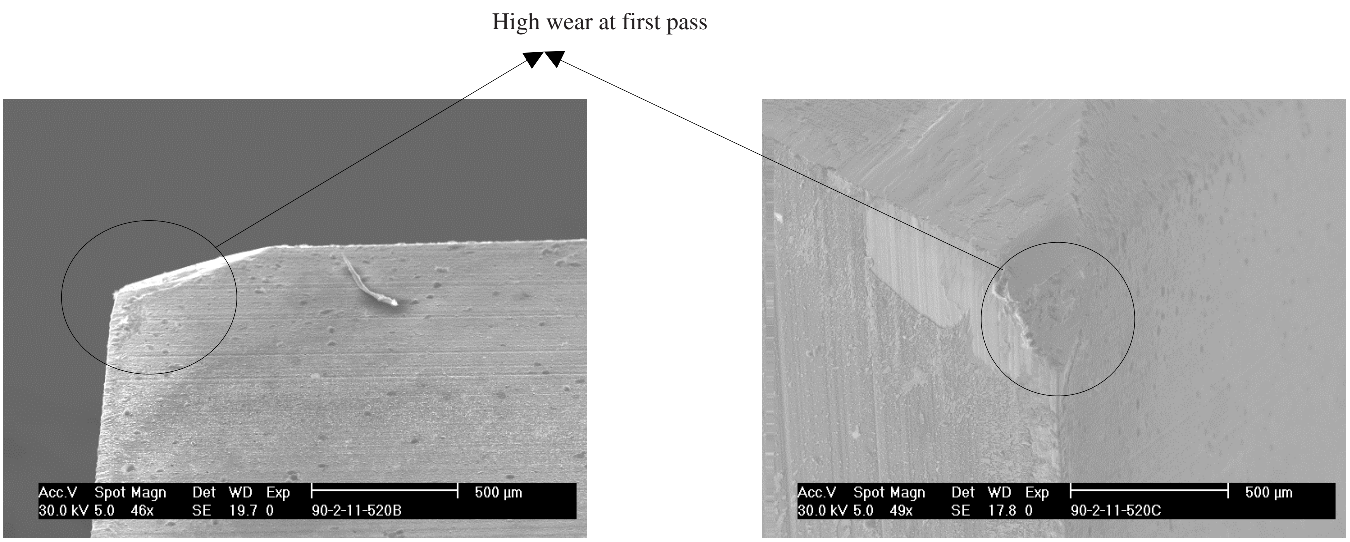

Fig. 2—SEM picture for cutting speed (Feed rate 0.15 mm/rev, axial depth 2 mm): Cutting speed 100 m/min

or limitations in material model at very large strain-rates[25]. Friction generated during machining is more complex indeed and advanced friction models based on chip-tool interface (CTI) conditions are needed[26]. Other studies also reported[27-30] similar problems associated with lack of friction models.

Comparisons between Three Prediction Values

Comparison between predicted values for cutting force, obtained by RSM, FEA and experimental data indicates that prediction values from two methods are in very close agreement with each other (Fig. 5). Looking into error percentage, RSM is found quite close to prediction value of FEA (Fig. 6). Thus, error for two techniques and RSM model can be accepted[22].

Optimization of Cutting Force Value

To minimize cutting force with correct combination of variables, in Minitab's approach to optimization, each of response values is transformed using a specific desirability function. For each response, a weight can be selected from 0.1-10 to emphasize or de-emphasize the target[31]. A weight (<1; minimum is 0.1) places less

Table 1—Experimental and prediction results for First order and Scond order cutting force model

Cutting speed m/min	Feed rate mm/rev	Axial depth mm	Exp. force N	Predicting cutting force (N) First Order Model	Predicting cutting force (N) Second Order Model
140	0.1	2	684	678.11	689.36
140	0.2	1	687	670.39	681.64
100	0.15	1	458.95	460.3	453.53
100	0.15	2	1050	1038.63	1039.48
140	0.15	1.5	685	674.25	685.67
100	0.1	1.5	449.51	464.16	454.67
180	0.1	1.5	310.54	313.74	299.76
180	0.15	2	876	888.2	881.42
180	0.2	1.5	880	884.34	874.84
140	0.2	2	1250	1248.71	1249.73
180	0.15	1	300.21	309.87	310.73
140	0.15	1.5	682	674.25	685.67
140	0.1	1	100.54	99.79	100.81
100	0.2	1.5	1010	1034.77	1020.79
140	0.15	1.5	690	674.25	685.67

Table 2—Variance analysis for First Order cutting force model

Source	DF	Seq SS	Adj SS	Adj MS	F	P
Regression	3	1365351	1365351	455117	2545.23	0
Linear	3	1365351	1365351	455117	2545.23	0
Residual error	11	1967	1967	179	-	-
Lack-of-fit	9	1934	1934	215	13.16	0.073
Pure error	2	33	33	16	-	-
Total	14	1367318	-	-	-	-

emphasis on target; a weight (=1) places equal importance on target and bounds, and a weight (>1; maximum is 10) places more emphasis on target. Optimum value for cutting speed can be achieved at 100.17 N that corresponds to design variable as: cutting speed, 180 m/min, feed rate, 0.1053 mm/rev; and axial depth, 1.0783 mm. This is minimum optimized value for selected range of variables parameters. It seems that cutting speed approaches to its maximum values, and feed rate and axial depth to minimum values.

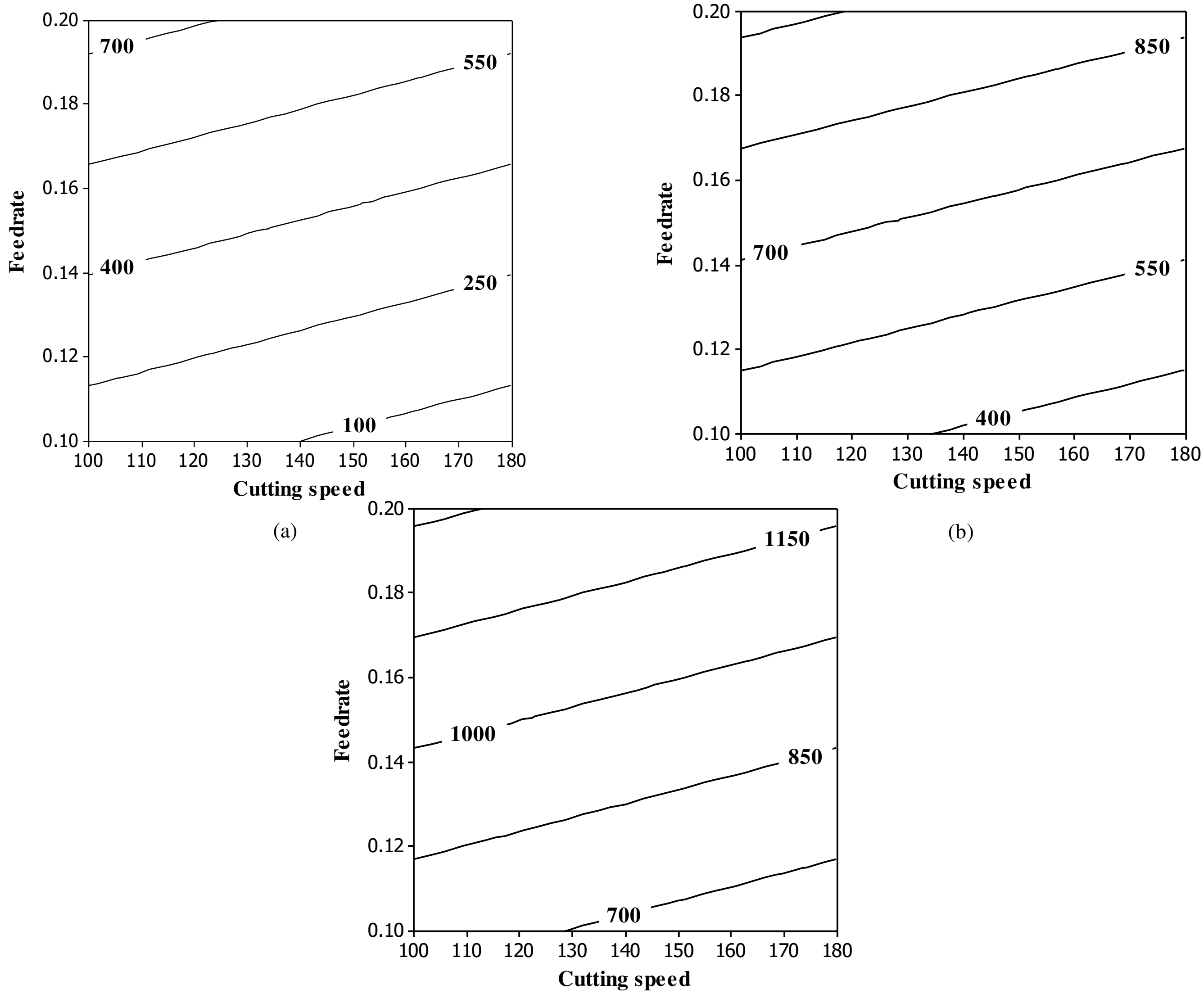

(a) (b) (c)

Fig. 3—Cutting force contours in cutting speed-feed rate plane for axial depth at: a) 1mm; (b) 1.5mm; (c) 2 mm

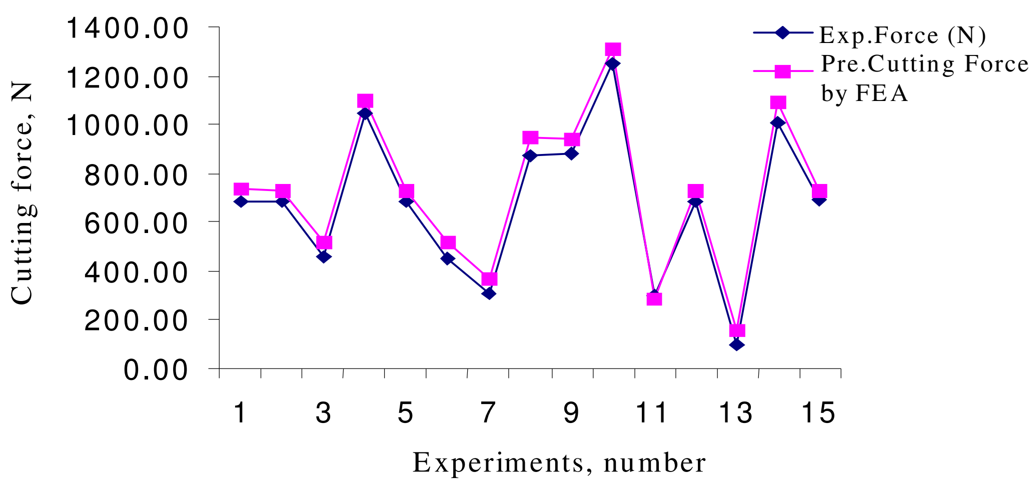

Fig. 4—Prediction of cutting force by finite element analysis (FEA) and experimental data

Table 3—Variance analysis for Second Order cutting force model

Source	DF	Seq SS	Adj SS	Adj MS	F	P
Regression	9	1366662	1366662	151851	1156.96	0
Linear	3	1365351	1365351	455117	3467.56	0
Square	3	1128	1128	376	2.86	0.143
Interaction	3	183	183	61	0.46	0.719
Residual error	5	656	656	131	-	-
Lack-of-Fit	3	624	624	208	12.73	0.074
Pure error	2	33	33	16	-	-
Total	14	1367318	-	-	-	-

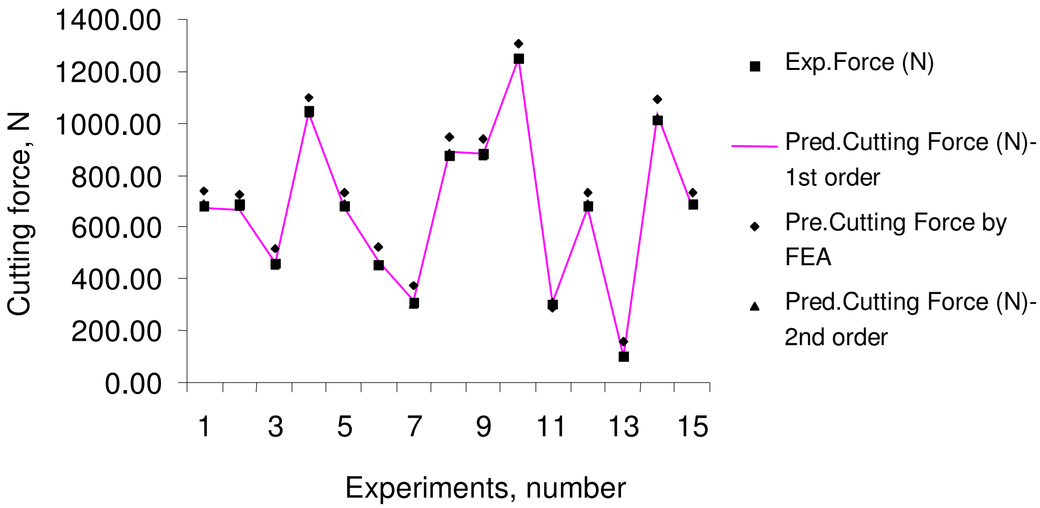

Fig. 5—Prediction of cutting force by three techniques used in this study

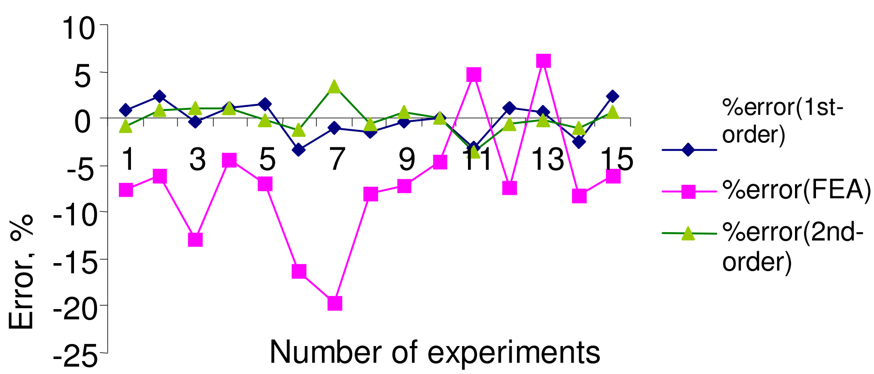

Fig. 6—Comparisons of error in prediction of cutting force by neural network (NN), Response surface method (RSM) and Finite Element Analysis (FEA)

Conclusions

RSM has been found successful technique to perform trend analysis of cutting force with respect to various combinations of three design variables (cutting speed, feed rate and axial depth). By using least square method, First- and Second-Order Models have been developed based on test conditions in accordance with Box-Behnken design method. The models have been found to accurately representing cutting force values with respect to experimental results, and simulated results using FEA. Both RSM models reveal that feed rate is most significant design variable in determining cutting force response as compared to others. In general, within the working range of variables, cutting force increases as feed rate and axial depth increases, while decreases when cutting speed increases. Based on Second-order RSM model, feed rate does not interact much with remaining design variables. With the model equations obtained, a designer can subsequently select best combination of design variables for achieving optimum cutting force.

Acknowledgement

Financial support by Malaysian Government through MOSTI and University Tenaga Nasional is gratefully acknowledged.

References

1 Haynes Hastelloy C-22HS Standard Product Catalogue (Haynes International,Indiana) 2007, 2-16.

2 Alauddin M, Mazid M A, EL Baradi M A & Hashmi M S J, Cutting forces in the end milling of Inconel 718, Mater Process Technol, **77** (1998) 153-159.

3 Trent E M, Metal Cutting, **3rd edn** (Butterworth-Heinemann, Jordan Hill) 1991, 236-248

4 Wuyi C, Cutting forces and surface finish when machining medium hardness steel using CBN tools, Inter Machine Tools Manuf, **40** (2000) 455-466

5 Koenigsberger F & Sabberwal A J P, An investigation into the cutting force pulsations during milling operations, Inter Mach Tool Design Res, **1** (1961) 15-33.

6 Kline W A, DeVor R E & Shareef I A, The prediction of surface accuracy in end milling, Trans ASME Engg Ind, **104** (1982) 272-278.

7 Kline W A, DeVor R E & Shareef I A, The effect of run out on cutting geometry and forces in end milling, Inter Mach Tool Design Res, **23** (1983) 123-140.

8 Sutherland J W & DeVor R E, "An improved method for cutting force and surface error prediction in flexible end milling systems", Trans ASME Engg Ind, **108** (1986) 269-279.

9 Budak E & Altintas Y, Peripheral milling conditions for improved dimensional accuracy, Inter Mach Tool Design Res, **34** (1994) 907-918.

10 Budak E & Altintas Y, Modeling and avoidance of static deformations in peripheral milling of plates, Inter Mach Tool Design Res, **35** (1995) 459-476.

11 Armarego E J A & Whitfield R C, Computer based modeling of popular machining operations for force and power predictions, Annals CIRP, **34** (1985) 65-69.

12 Zorev N N, Metal Cutting Mechanics (Pergamon Press, Britain) 1966, 30-56.

13 Taylor F W, On the art of cutting metals, Trans ASME, **28** (1952), 31-35.

14 Victor H, Beitrag zur Kenntnis der Schnittkraft beim Drehen, Hobeln und Bohren, Diss., TH Hannover, 1956, 39.

15 Victor H, Schnittkraftberechnung fu¨r das Abspanen von Metallen, Wt-Z Ind Fert, **59** (1969) 317-327.

16 Kienzle O, Die Bestimmung von Kra¨ften und Leistungen an spa¨nenden Werkzeugen und Werkzeugmaschinen, Z. VDI, **94** (1952) 299-305.

17 Douglas C.Montgomery; Design and Analysis of Experiments, **5th edn** (John Wiley & Sons, USA) 1997,58-72.

18 Andre I K & John A C, Response Surfaces Design and Analyses **2nd edn** (Marcel Dekker, Inc, New York) 1988, 112-124.

19 Boothroyd G, Fundamentals of Metal Machining and Machine Tools (McGraw Hill Publishers, Columbus) 1975, 202-250.

20 Third Wave System AdvantEdge User Manual Version 4.8 (Third Wave System, Minneapolis) 2007, 8-20.

21 Haci S, Suleyman Y & Faruk U, The effect of tool geometry and cutting speed on main cutting force and tool tip temperature, Mater Design (in press).

22 Abou-El-Hossein K A, Kadirgama K, Hamdi M & Benyounis K Y, Prediction of cutting force in end-milling operation of modified AISI P20 tool steel, Mater Process Technol, **182** (2007) 241-247.

23 Li H Z, Zeng H & Chen X O, An experimental study of tool wear and cutting force variation in the end-miliing of Inconel 718 with coated carbide inserts, Mater Process Technol (in press).

24 Abhijeet S M, Wenping J, Brown W D & Ajay P M, Tool wear and machining performance of cBN–TiN coated carbide inserts and PCBN compact inserts in turning AISI 4340 hardened steel, Mater Process Technol (in press).

25 Tugrul O, Modelling of hard part machining:Effect of insert edge preparation in CBN cutting tools, Mater Process Technol, **141** (2003) 284-293.

26 Bhattacharya S & Lovell M R, Characterization of friction in machining: evaluation of asperity deformation and seizure-based models, Trans NAMRI/SME, **XXVII** (2000) 107-112.

27 Ceretti E, Lucchi M & Altan T, Finite element simulation of orthogonal cutting: serrated chip formation, Mater Process Technol, **95** (1999) 17-26.

28 Ng E G, Aspinwall D K, Brazil D & Monaghan J, Modelling of temperature and forces when orthogonally machining hardened steel, Int J Mach Tools Manuf, **39** (1999) 885-903.

29 Guo Y B & Liu C R, 3D FEA modeling of hard turning, ASME J Manuf Sci Engg, **124** (2002) 189-199.

30 Movahhedy M R, Altintas Y & Gadala M S, Numerical analysis of cutting with chamfered and blunt tools, ASME J Manuf Sci Eng, **124** (2002) 178-188.

31 Minitab User Manual Version 14 (Minitab Inc.USA) 2005, 50-72.